Short communication

Synthesis and electrochemical characterization of spinel Li[Li$_{(1−x)/3}$Cr$_x$Ti$_{(5−2x)/3}$]O$_4$ anode materials

Y.-K. Sun [a,*], D.-J. Jung [a], Y.S. Lee [b], K.S. Nahm [c]

[a] *Department of Chemical Engineering, Hanyang University, Seongdong-Gu, Seoul 133-791, South Korea*
[b] *Faculty of Applied Chemical Engineering, Chonnam National University, Kwangju 500-757, South Korea*
[c] *School of Chemical Engineering and Technology, Chonbuk National University, Chonju 561-756, South Korea*

Abstract

Spinel Li[Li$_{(1−x)/3}$Cr$_x$Ti$_{(5−2x)/3}$]O$_4$ compounds have been investigated as anode materials for lithium secondary batteries. Li[Li$_{(1−x)/3}$Cr$_x$Ti$_{(5−2x)/3}$]O$_4$ electrodes ($0 \le x \le 1.0$) exhibit a reversible capacity between 163 and 154 mAh g^{-1} with excellent cycleability. Increase in the amount of Cr ions substituted for Ti ions in the spinel structure decreases the reversible capacity due to a smaller theoretical capacity, but lowers the area specific impedance (ASI) and increases the rate capability.
© 2003 Elsevier B.V. All rights reserved.

Keywords: Lithium secondary batteries; Spinel; Area specific impedance; Rate capability; Chromium; Titanium

1. Introduction

Spinel Li[Li$_{1/3}$Ti$_{5/3}$]O$_4$ is the end member of the solid solution of Li$_{1+x}$Ti$_x$O$_4$ ($0 \le x \le 1/3$). The compound has a cubic structure with a space group symmetry $Fd\bar{3}m$ in which lithium-ions are located at tetrahedral 8a sites. Titanium and lithium-ions are randomly distributed at octahedral 16c sites in the spinel notation as Li$_{8a}$[Li$_{1/3}$Ti$_{5/3}$]$_{16d}$O$_4$. As lithium-ions are inserted into the spinel structure, those at tetrahedral 8a sites cooperatively move into neighboring 16c octahedral sites, and yield the rock-salt phase {Li$_2$}$_{16c}$[Li$_{1/3}$Ti$_{5/3}$]$_{16d}$O$_4$ [1,2]. During this reduction process from Li[Li$_{1/3}$Ti$_{5/3}$]O$_4$ to Li$_2$[Li$_{1/3}$Ti$_{5/3}$]O$_4$, the Li[Li$_{1/3}$Ti$_{5/3}$]O$_4$ spinel electrode shows a voltage plateau of approximately 1.5 V versus Li/Li$^+$. Although the potential of the Li[Li$_{1/3}$Ti$_{5/3}$]O$_4$ electrode is rather high compared with the carbon electrode, some research groups have tried to make 2.2 and 3.2 V lithium-ion cells combined with 4 V (LiCoO$_2$ and LiMn$_2$O$_4$) and 5 V cathode materials (LiNi$_{0.5}$Mn$_{1.5}$O$_4$) with improved safety features.

It is well known that the cycleability of electrodes used in lithium secondary batteries greatly depends on the structural stability of the host materials during the charge-discharge process. Li[Li$_{1/3}$Ti$_{5/3}$]O$_4$ shows excellent cycling behavior because the change in the cell volume is less than 1% during cycling [2]. On the other hand, the electronic conductivity of the material is extremely low due to its insulator properties. In order to enhance the electrical conductivity of these materials, Chen et al. [3] reported that the substitution of Mg^{2+} ions for Li$^+$ ions in the structure, i.e., Li$_{4-x}$Mg$_x$Ti$_5$O$_{12}$ with mixed Ti^{3+}/Ti^{4+} valence, increases the conductivity by many orders of magnitude from $\sigma < 10^{-13}$ to $\sigma = 10^{-2}$ S cm^{-1}, but with same sacrifice of capacity [3]. Robertson et al. [4,5] reported the effect on the electrochemistry of Li$_4$Ti$_5$O$_{12}$ by replacing some of Ti^{4+} with M^{3+} transition metals (3M$^{3+} = 2$Ti$^{4+} +$ Li$^+$, M = Fe, Cr, Ni) [4,5]. The principal interest of that work was to investigate low-voltage materials at less than 1 V versus Li/Li$^+$.

In this study, Li[Li$_{(1−x)/3}$Cr$_x$Ti$_{(5−2x)/3}$]O$_4$ has been synthesized by the sol–gel method and the effect of the amount of Cr substitution for Li and Ti on the structural and electrochemical properties of Li[Li$_{(1−x)/3}$Cr$_x$Ti$_{(5−2x)/3}$]O$_4$ have been studied.

2. Experimental

Li[Li$_{(1−x)/3}$Cr$_x$Ti$_{(5−2x)/3}$]O$_4$ ($0 \le x \le 1.0$) powders were synthesized according to the procedure shown in Fig. 1. A stoichiometric amount of lithium acetate (Li(CH$_3$COO)·2H$_2$O), chromium nitrate (Cr(NO$_3$)$_3$·9H$_2$O),

* Corresponding author. Tel.: +82-2-2290-0524; fax: +82-2-2282-7329.
E-mail address: yksun@hanyang.ac.kr (Y.-K. Sun).

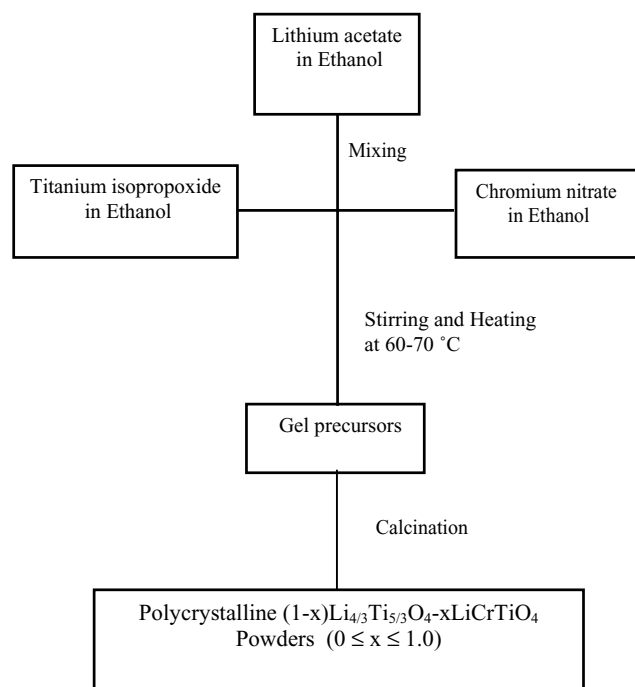Fig. 1. Flowsheet of procedure for preparing polycrystalline Li[Li$_{(1-x)/3}$Cr$_x$Ti$_{(5-2x)/3}$]O$_4$ powders.

Fig. 2. X-ray diffraction (XRD) patterns for Li[Li$_{(1-x)/3}$Cr$_x$Ti$_{(5-2x)/3}$]O$_4$ powders calcined at 800 °C for 12 h, x in (a) 1, (b) 0.6, and (c) 0.

and titanium isopropoxide (Ti(OCH(CH$_3$)$_2$)$_4$) salts with cationic ratio of Li:Ti:Cr $= (4 - x)/3$:x:$(5 - 2x)/3$ ($x = 0$, 0.2, 0.4, 0.6, 1.0) was dissolved in absolute ethanol and mixed well. The resultant solution was evaporated at 60–70 °C for 5 h until a transparent sol was obtained. As the ethanol was evaporated further, the sol turned into a viscous transparent gel. The gel precursors obtained were decomposed at 450 °C in air for 5 h and calcined at 800 °C for 12 h.

Powder X-ray diffraction (XRD, Rigaku, Rint-2000) using Cu Kα radiation was used to characterize the structural properties of the synthesized powders. Rietveld refinement was then performed on the XRD data to obtain the lattice constants. Charge–discharge cycles were performed with CR2032 coin type cells. The cell consisted of a cathode and a lithium metal anode which were separated by a porous polypropylene film. For the fabrication of the electrode, a mixture of 20 mg of Li[Li$_{(1-x)/3}$Cr$_x$Ti$_{(5-2x)/3}$]O$_4$ powder and 12 mg conducting binder (8 mg Teflonized acetylene black (TAB) and 4 mg of graphite) was pressed on to a 2.0 cm^2 copper screen at 500 kg cm^2. The electrolyte was a 1:1 (v/v) mixture of ethylene carbonate (EC) and dimethyl carbonate (DMC) and contained 1 M LiPF$_6$. Charge–disharge cycling was carried out galvanostatically at a current rate of 0.2 mA cm^{-2} (20 mA g^{-1}) at 30 °C in the voltage range 1.2–3.0 V. The chemical diffusion coefficient of lithium ions in Li[Li$_{(1-x)/3}$Cr$_x$Ti$_{(5-2x)/3}$]O$_4$ cathodes was determined by the galvanostatic intermittent titration technique (GITT).
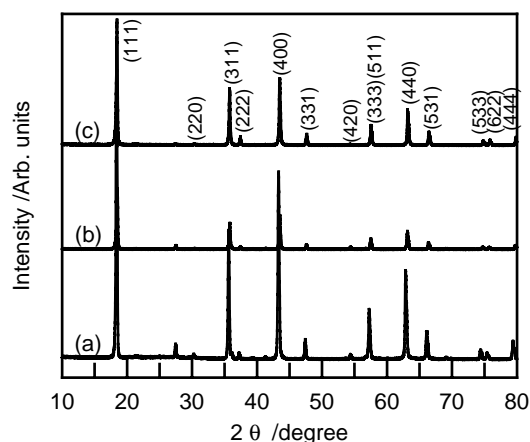
3. Results and discussion

XRD patterns for the Li[Li$_{(1-x)/3}$Cr$_x$Ti$_{(5-2x)/3}$]O$_4$ ($x = 0$, 0.6, 1) powders calcined at 800 °C for 12 h are shown in Fig. 2. All the diffraction peaks can be indexed based on a spinel structure with space $Fd\bar{3}m$. A small amount of TiO$_2$ with a peak at $2\theta = 27.5°$ is also observed. It is evident from the XRD data that the Cr cations are located at the octahedral site (16c), i.e., there is no change of the (2 2 0) peak at approximately $2\theta = 30.2°$ due to low scattering factor of lithium atom at the tetrahedral (8a) site. This is consistent with the structural analysis of Li$_{8a}$[CrTi]$_{16d}$O$_4$ by Ohzuku et al. [6]. Since the ionic radius of Cr^{3+} ($r_{Cr}^{3+} = 0.62$ Å) is nearly the same as to that of Ti^{4+} ($r_{Ti}^{4+} = 0.61$ Å), Cr ions are easily incorporated in the octahedral sites [7]. Fig. 3 shows the dependence of the lattice constant of the cubic unit cell on x, where x is the Cr content in the Li[Li$_{(1-x)/3}$Cr$_x$Ti$_{(5-2x)/3}$]O$_4$ powder. It is seen that the lattice constant decreases linearly up to 8.308 Å with increasing Cr content.

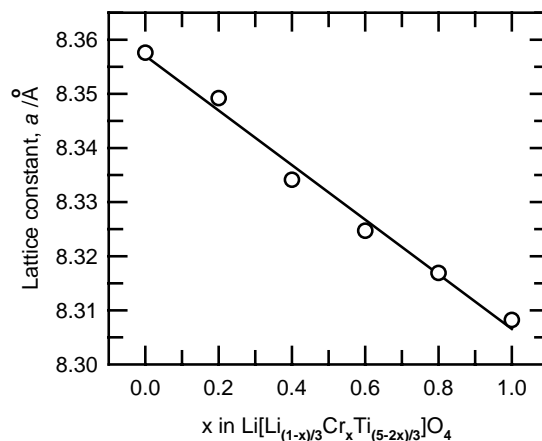Fig. 3. Dependence of lattice constant a of Li[Li$_{(1-x)/3}$Cr$_x$Ti$_{(5-2x)/3}$]O$_4$ powders on Cr content (x).
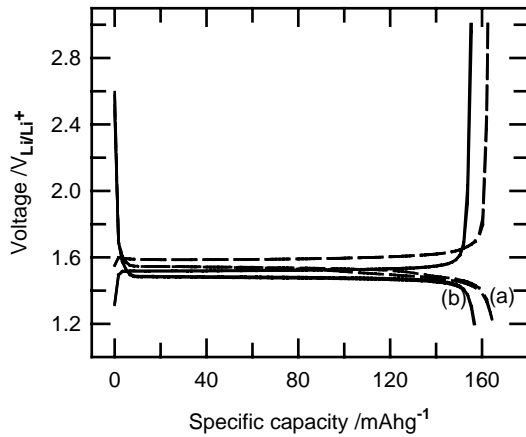
Fig. 4. Charge–discharge curves of (a) Li/Li[Li$_{1/3}$Ti$_{5/3}$]O$_4$ and (b) Li/Li[CrTi]O$_4$ cells.

Fig. 6. Area specific impedance (ASI) of Li/Li[Li$_{(1-x)/3}$Cr$_x$Ti$_{(5-2x)/3}$]O$_4$ cells ($x = 0$, 0.6, 1) as function of state-of-discharge (SOD).

A comparison between the charge–discharge curves of Li/Li[Li$_{1/3}$Ti$_{5/3}$]O$_4$ and Li/Li[CrTi]O$_4$ cells is given in Fig. 4. The operating voltage of the Li/Li[Li$_{1/3}$Ti$_{5/3}$]O$_4$ cell is 50 mV higher than that of the Li/Li[CrTi]O$_4$ cell, which is consistent with the results of a previous study [6]. The cycling behavior of the Li/Li[Li$_{(1-x)/3}$Cr$_x$Ti$_{(5-2x)/3}$]O$_4$ ($x = 0$, 0.6, 1) cells is reported in Fig. 5. The Li[Li$_{1/3}$Ti$_{5/3}$]O$_4$ and Li[CrTi]O$_4$ electrodes deliver 164 and 156 mAh g^{-1}, respectively. The Li[Li$_{(1-x)/3}$Cr$_x$Ti$_{(5-2x)/3}$]O$_4$ ($x = 0$, 0.6, 1) electrodes show an excellent cycleability with >99% capacity retention up to 50 cycles. The lower discharge capacity of the Li[CrTi]O$_4$ electrode is attributed to the reduced theoretical capacity. The theoretical capacities for Li[Li$_{1/3}$Ti$_{5/3}$]O$_4$ and Li[CrTi]O$_4$ are 175 and 157 mAh g^{-1}, respectively.

The area specific impedance (ASI) is directly related to power capability of a battery. Fig. 6 shows the ASI as a function of state-of-discharge (SOD) for Li/Li[Li$_{(1-x)/3}$Cr$_x$Ti$_{(5-2x)/3}$]O$_4$ cells ($x = 0$, 0.6, 1). The ASI was determined as $(A \Delta V)/I$, where A is the cross-sectional area,

ΔV is the voltage variation during current interruption for 60 s at each SOD, and I is the current applied during the galvanostatic cycling. Whereas Li[Li$_{1/3}$Ti$_{5/3}$]O$_4$ and Li[Li$_{0.133}$Cr$_{0.6}$Ti$_{1.267}$]O$_4$ electrodes exhibit ASI values of 25 to 40 and 24 to 40 Ω cm^2 at 20–60% SOD, respectively, the Li[CrTi]O$_4$ electrode displays a smaller value of 22 to 31 Ω cm^2. The smaller ASI of the Li[CrTi]O$_4$ electrode is partly attributed to enhancement of the electrical conductivity that results from a mixed-valence effect between Cr^{3+} and Ti^{4+}.

The discharge capacity of Li/Li[Li$_{(1-x)/3}$Cr$_x$Ti$_{(5-2x)/3}$]O$_4$ cells ($x = 0$, 0.6, 1) at various C rates is presented in Fig. 7. The different current densities were applied progressively for five cycles. The discharge capacities of the Li[CrTi]O$_4$ electrode fall to 127 mAh g^{-1} at the 1C rate and 88 mAh g^{-1} at the 2C rate from 153 mAh g^{-1} at the 0.2C rate. By contrast the discharge capacities of the Li[Li$_{1/3}$Ti$_{5/3}$]O$_4$ and Li[Li$_{0.133}$Cr$_{0.6}$Ti$_{1.267}$]O$_4$ electrodes decrease rapidly at the 1C and 2C rates. The discharge capacity of the Li[CrTi]O$_4$ electrode at the 2C rate is twice as large as that of the
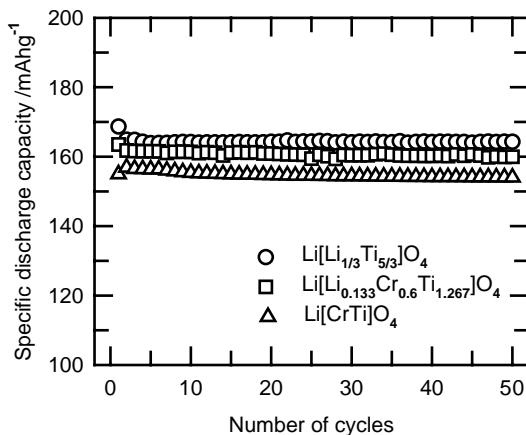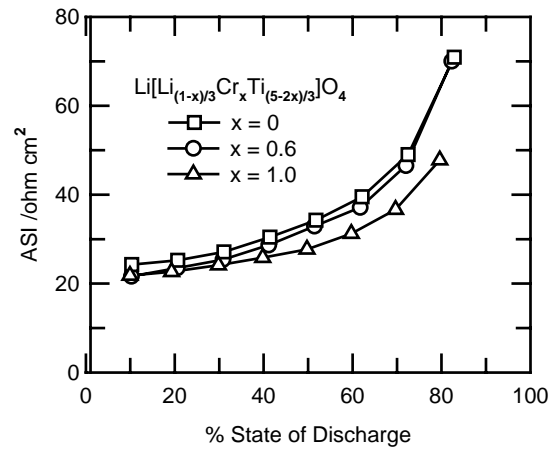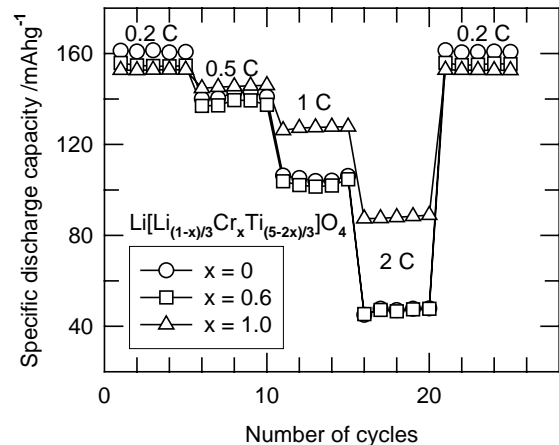

Fig. 5. Variation of specific discharge capacities with cycle number of Li/Li[Li$_{(1-x)/3}$Cr$_x$Ti$_{(5-2x)/3}$]O$_4$ ($x = 0$, 0.6, 1) cells.

Fig. 7. Variation of discharge capacities of Li[Li$_{(1-x)/3}$Cr$_x$Ti$_{(5-2x)/3}$]O$_4$ cells ($x = 0$, 0.6, 1) at various C rates.
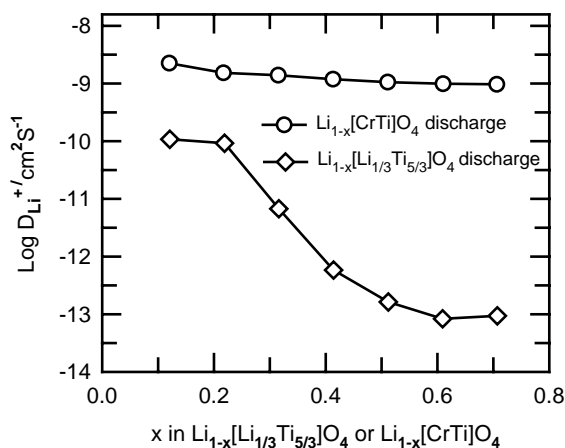
Fig. 8. Variation of $\tilde{D}_{Li}^+$ values in Li[Li$_{1/3}$Ti$_{5/3}$]O$_4$ and Li[CrTi]O$_4$ electrodes as function of lithium composition, x, during discharge process.

Li[Li$_{1/3}$Ti$_{5/3}$]O$_4$ electrode, which is well consistent with the ASI values.

Fig. 8 shows the variation of the $\tilde{D}_{Li}^+$ values, the chemical diffusion coefficient of lithium ions in Li[Li$_{1/3}$Ti$_{5/3}$]O$_4$ and Li[CrTi]O$_4$ electrodes, as a function of lithium composition, x, during the discharge process. Based on the crystal structure of the Li[Li$_{(1-x)/3}$Cr$_x$Ti$_{(5-2x)/3}$]O$_4$ phase, the intercalation process is partly controlled by the number of ion occupancies in the host lattice, whereas the de-intercalation process in the Li[Li$_{1/3}$Ti$_{5/3}$]O$_4$ electrode is strongly dependent on the concentration of Ti^{3+} ions. The magnitude of the diffusion coefficient of lithium-ions for Li[CrTi]O$_4$ is around 10^{-9} cm^2 s^{-1}. By contrast, the diffusion coefficient for Li[Li$_{1/3}$Ti$_{5/3}$]O$_4$ rapidly decreases with decreasing Li content (Ti^{3+} concentration) and falls to 10^{-13} cm^2 s^{-1}. The improved lithium diffusivity and the enhancement of electrical conductivity of the Li[CrTi]O$_4$ electrode lower the ASI, but increase the rate capability.

4. Conclusions

Li[Li$_{(1-x)/3}$Cr$_x$Ti$_{(5-2x)/3}$]O$_4$ materials have been synthesized by a sol–gel method and have been characterized as anode materials for lithium secondary batteries. Increase in the amount of Cr ions substituted for Ti ions in the spinel structure decreases the reversible capacity due to the smaller theoretical capacity. On the other hand, this substitution lowers the ASI and increases the rate capability. Li[Li$_{(1-x)/3}$Cr$_x$Ti$_{(5-2x)/3}$]O$_4$ electrodes ($0 \leq x \leq 1.0$) exhibit a reversible capacity between 163 and 154 mAh g^{-1} with good cycleability.

Acknowledgements

References

[1] T. Ohzuku, A. Ueda, N. Yamamoto, J. Electrochem. Soc. 142 (1985) 1431.
[2] S. Scharner, W. Weppner, P. Schmid-Beurmann, J. Electrochem. Soc. 146 (1999) 857.
[3] C.H. Chen, J.T. Vaughey, A.N. Jansen, D.W. Dees, A.J. Kahaian, T. Goacher, M.M. Thackeray, J. Electrochem. Soc. 148 (2001) A102.
[4] A.D. Robertson, L. Trevino, H. Tukamoto, J.T.S. Irvine, J. Power Sources 81–82 (1999) 352.
[5] A.D. Robertson, H. Tukamoto, J.T.S. Irvine, J. Electrochem. Soc. 146 (1999) 3958.
[6] T. Ohzuku, K. Tatsumi, N. Matoba, K. Sawai, J. Electrochem. Soc. 47 (2000) 3592.
[7] R.D. Shannon, C.T. Prewitt, Acta Crystallogr. B26 (1970) 1046.